ACS Catalysis

pubs.acs.org/acscatalysis Research Article

Highly Selective Oxidation of Methane into Methanol over Cu-Promoted Monomeric Fe/ZSM-5

Tao Yu,[†] Zhi Li,[†] Lu Lin, Shengqi Chu, Yang Su, Weiyu Song,* Aiqin Wang, Bert M. Weckhuysen,* and Wenhao Luo*

Cite This: *ACS Catal.* 2021, 11, 6684–6691 Read Online

ACCESS | Metrics & More | Article Recommendations | Supporting Information

ABSTRACT: The selective oxidation of methane into methanol is of paramount importance but poses significant challenges in achieving high methanol productivity and selectivity, especially under mild reaction conditions. We show that a Cu-modified monomeric Fe/ZSM-5 catalyst is a highly efficient material for the direct conversion of methane into methanol in the liquid phase using H_2O_2 as an oxidant at low temperatures, which exhibits an excellent methanol productivity of 431 $mol_{MeOH}{\cdot}mol^{-1}_{Fe}{\cdot}h^{-1}$ (with a methanol selectivity of ~80% over the Cu-Fe(2/0.1)/ZSM-5 catalyst). Combining the control experiments and comprehensive characterization results by among others, Mössbauer spectroscopy, and electron paramagnetic resonance as well as density functional theory calculations, we found that Cu species in the Cu-Fe(2/0.1)/ZSM-5 catalyst play a pivotal role in facilitating the formation of •OH radicals, which quickly react with $•CH_3$ radicals to form CH_3OH. These findings provide valuable insights into the rational design of metal−zeolite combinations for the selective oxidation of methane into methanol.

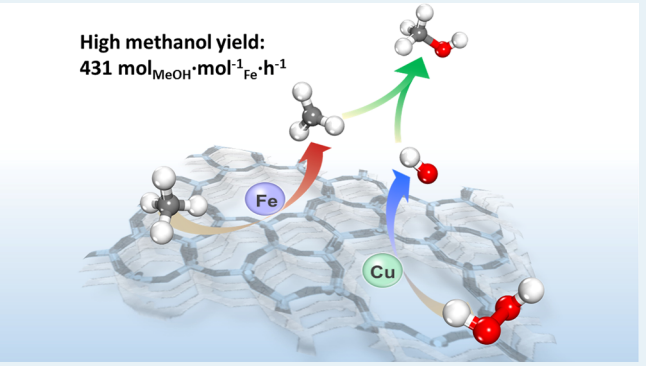

KEYWORDS: *copper, characterization, monomeric Fe species, methane, zeolite*

INTRODUCTION

The selective oxidation of methane, the major constituent of natural gas, remains a great challenge and has attracted significant research interest over decades.[1−3] In current industries, methane is used for methanol production in an energy-intensive two-step process via the intermediate use of synthesis gas (CO/H_2 mixture).[4−6] The direct, selective oxidation of methane into methanol poses great challenges, arising from the activation of the stable C−H bonds and efficient suppressing the facile, consecutive overoxidation of primary oxygenates. The direct approach of methane utilization would show significant advantages.[7−9] Inspired by the biocatalytic systems developed over millions of years in nature,[10,11] metal-containing zeolite systems with the mimicof the enzymelike active Fe-oxo or Cu-oxo active sites have received great attention and are being extensively studied.[12−17] Of particular interest is the low-temperature approach, as pioneered by Hutchings et al.,[18] utilizing Cu-Fe/ZSM-5 as a catalyst and H_2O_2 as an oxidant under aqueous conditions. Fe species, instead of Cu species, were reported as the key active component in Cu-Fe/ZSM-5 for methane activation. A high turnover rate (TOR) of 31 $mol_{MeOH}{\cdot}mol^{-1}_{Fe}{\cdot}h^{-1}$ with a high methanol selectivity of ~85% can be achieved with a state-of-the-art bimetallic catalyst. They proposed that the positive role of Cu species in enhancing methanol selectivity was attributed to the elimination of •OH radicals, which facilitated the overoxidation of methanol into formic acid. However, this is unusual and contradicted the typical observation that the interaction between Cu species and H_2O_2 can produce •OH radicals.[19−21] As such, the role of Cu species in Cu-Fe/ZSM-5 for the low-temperature methane oxidation remains ambiguous and under debate.

We have previously discovered that monomeric 0.1Fe/ZSM-5, presenting a much higher efficiency in methanol production than the other counterpart species, is the intrinsic active site for low-temperature methane oxidation.[22] Still, the control of high selectivity to methanol is difficult to be achieved for this monomeric 0.1Fe/ZSM-5 catalyst system as the overoxidation of methanol to formic acid cannot be efficiently suppressed. In this work, we further explore the Cu-modified monomeric Fe/ZSM-5 catalyst material for the selective oxidation of methane into methanol. We have systematically studied the influence of Cu species on the activity and selectivity of this material. It was

Received: February 25, 2021
Revised: April 27, 2021
Published: May 21, 2021

https://doi.org/10.1021/acscatal.1c00905
ACS Catal. 2021, 11, 6684–6691

Table 1. Comparison of Catalytic Performances for the as-Prepared Catalyst Materials and Reported Fe-Containing Catalyst Materials[e]

		C1 products (mol/mol$_{Fe}$)							
catalyst material	Fe (wt %)	CH_3OH	CH_3OOH	$HOCH_2OOH$	HCOOH	CO_2	TOR (h^{-1})[a]	CH_3OH sel. (%)[b]	ref
Cu-Fe(0.1/0.1)/ZSM-5	0.1	66.8	25.9	31.7	113.3	10.3	134	27	this work
Cu-Fe(0.5/0.1)/ZSM-5	0.1	169.9	20.2	30.4	118.5	6.9	340	49	this work
Cu-Fe(1/0.1)/ZSM-5	0.1	209.4	18.5	28.6	84.6	9.3	419	60	this work
Cu-Fe(2/0.1)/ZSM-5	0.1	215.6	16.6	29.7	0.0	9.1	431	80	this work
Cu-Fe(3/0.1)/ZSM-5	0.1	160.9	15.3	26.5	0.0	8.6	322	76	this work
Fe/ZSM-5	2.5	1.9	0.1	NA	13.6	3.2	4	10	18
Cu-Fe/ZSM-5	2.5	15.7	0.0	NA	0.0	2.8	31	85	18
Fe/ZSM-5	0.1	33.0	46.3	35.7	80.5	5.8	66	16	22
FeN_4/GN[c]	2.7	0.2	1.7	1.3	1.5	0.3	0.02	5	23
Fe/ZSM-5	2.5	1.5	0.2	NA	7.3	2.8	3	13	24
Cu(1.25)Fe/ZSM-5	1.25	22.4	NA	NA	NA	6.4	45	78	24
Fe/ZSM-5	0.5	8.3	3.4	NA	23.0	5.9	17	20	25
Fe-UiO-66[d]	2.2	0.7	1.0	2.6	7.9	0.3	0.7	5	26

[a]TOR is defined as mole (methanol)/mole (Fe)/time. [b]Methanol selectivity is calculated as moles (CH_3OH)/moles (produced) × 100. [c]Reaction conditions: 25 °C, 20 bar CH_4 (89.9%, N_2 as balance gas), 10 h. [d]Reaction condition: 1 h. [e]NA: not available.

found that the optimal Cu-Fe(2/0.1)/ZSM-5 catalyst, containing dominant mononuclear Fe species, exhibits an excellent methanol productivity of 431 $mol_{MeOH}·mol^{-1}_{Fe}·h^{-1}$, which is at least an order of magnitude higher than that of any previously reported catalyst. The role of Cu species has been elucidated and it was found that Cu species not only promote methanol formation by generating •OH radicals but also efficiently suppress the formation of formic acid. Relatedly, a reaction mechanism is proposed based on a.o., spectroscopic data, and density functional theory (DFT) calculations.

RESULTS AND DISCUSSION

To explore the impact of Cu species on catalytic activity and selectivity (Table 1), a series of Cu-Fe/ZSM-5 catalyst materials with different Cu loadings from 0.1 to 3 wt % has been prepared using the coimpregnation method. The catalytic oxidation of methane using H_2O_2 was conducted in a batch system at 50 °C with 30 bar of CH_4 and 0.5 M H_2O_2. Notably, the as-prepared Cu-Fe/ZSM-5 catalysts show significant activity for the selective oxidation of methane into methanol (Table 1, entries 1−5). In particular, the Cu-Fe(2/0.1)/ZSM-5 catalyst affords the maximum methanol yield of 215.6 mol/mol_{Fe} at a reaction time of 30 min, together with no formation of formic acid observed (Table 1, entry 4). Considering that a trace amount of Fe species within zeolite ZSM-5 can afford activity, silicalite-1-supported Cu or Fe catalysts, with the exclusion of Fe impurity in the zeolite structure, were also prepared and compared (Figure S1). Adding Fe into inactive silicalite-1 can significantly enhance the activity, while adding Cu into silicalite-1 provides limited contribution to activity. This strongly suggests that the key active component for methane activation under low-temperature, liquid-phase conditions is Fe species, instead of Cu species, an observation which is consistent with earlier reported results.[18,23] To evaluate the methanol productivity for this reaction, the TOR was defined as the number of moles of methanol formed per hour and per mole of Fe in the catalyst. The optimal Cu-Fe(2/0.1)/ZSM-5 catalyst, possessing an excellent TOR of 431 h^{-1} and a methanol selectivity of 80%, shows a unique level of activity and selectivity. This TOR value is about one order of magnitude higher than that of the state-of-the-art Cu-Fe/ZSM-5[24] catalyst (Table 1, entry 11). Although many other works showed an apparently high methanol selectivity of >80%, it should be noted that those selectivity values may be affected by the often missing intermediates or lack of counting of some intermediates, such as CH_3OOH and $HOCH_2OOH$.

To unravel the structure−performance relationship for this catalyst system, we focused our attention on the study of the optimal Cu-Fe(2/0.1)/ZSM-5 catalyst by employing a series of characterization methods, namely, X-ray diffraction (XRD), scanning transmission electron microscopy−energy-dispersive X-ray spectroscopy (STEM-EDX), UV−vis diffuse reflectance spectroscopy (DRS), Mössbauer spectroscopy, and X-ray photoelectron spectroscopy (XPS). The XRD pattern of the Cu-Fe(2/0.1)/ZSM-5 catalyst shows no observed metal species, indicating good dispersion of Fe and Cu species (Figure S2). STEM-EDX reveals that the majority of Fe and Cu species are highly dispersed, together with some Cu nanoparticles in the 2−10 nm size range on the external surface of the zeolite ZSM-5 (Figure 1 and Figure S3). UV−vis DRS further corroborates the findings observed by STEM (Figure 2a). In the UV−vis DR spectrum of the Cu-Fe(2/0.1)/ZSM-5 sample, two major signals are observed. One sharp absorption band at ∼203 nm is ascribed to isolated Cu^{2+} species, while another broad band at ∼269 nm may correspond to a combined contribution of mononuclear Fe^{3+} species in octahedral coordination and isolated Cu^{+} species.[27−30] The absence of absorption bands in the spectral range of 300−450 nm indicates the absence of oligomeric Fe/Cu species.[27,29,30] A close inspection of the UV−vis DR spectrum of the Cu-Fe(2/0.1)/ZSM-5 sample at above 600 nm range shows a broad weak band indicative of the coexistence of CuO nanoparticles (Figure 2a). For the monometallic catalysts, the 0.1Fe/ZSM-5 sample shows only one absorption band at ∼270 nm, corresponding to the presence of mononuclear Fe^{3+} in an octahedral coordination.[29,30] The 2Cu/ZSM-5 sample has a similar spectrum as the Cu-Fe(2/0.1)/ZSM-5 sample but with a lower amount of isolated metal species and more CuO nanoparticles, as also evidenced by STEM.

Further validation and quantification of the different Fe species in the samples have been accomplished by ^{57}Fe Mössbauer spectroscopy (Figure 2b). The isomer shift (IS) and quadrupole splitting (QS) obtained by spectral deconvolution are listed in Table S1. Two doublet species can be

https://doi.org/10.1021/acscatal.1c00905
ACS Catal. 2021, 11, 6684−6691

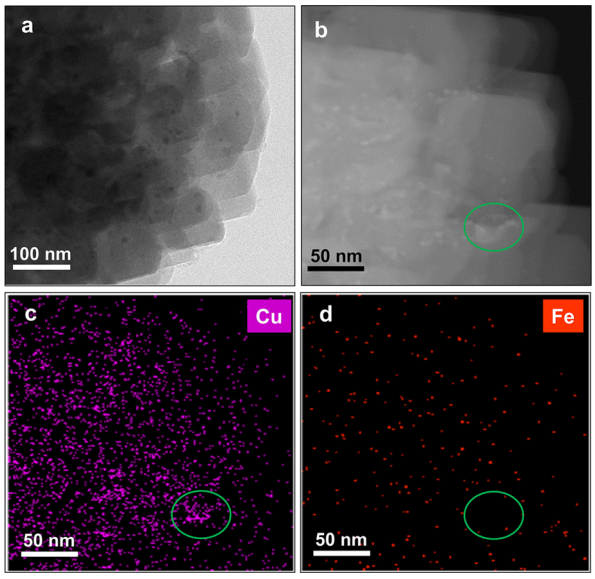

Figure 1. (a,b) STEM image of the Cu-Fe(2/0.1)/ZSM-5 catalyst at different magnifications and (c,d) EDX mapping images of the Cu-Fe(2/0.1)/ZSM-5 catalyst in panel (b).

identified for both the 0.1Fe/ZSM-5 and Cu-Fe(2/0.1)/ZSM-5 catalysts. One doublet with IS = 0.36 and QS = 0.69∼0.70 mm/s could be assigned to the dominant monomeric Fe^{3+} species in an octahedral coordination. The other doublet with IS = 0.34∼0.38 and QS = 1.47∼1.55 mm/s was assigned to oligomeric Fe_xO_y species ($x \geq 2$) in a strongly distorted octahedral environment. Notably, adding Cu into the 0.1Fe/ZSM-5 catalyst leads to an increase of proportion of isolated monomeric Fe^{3+} species from 66 to 71% (Table S1). From our previous study,[22] we found that the catalytic activity was exponentially related to the proportion of the active monomeric Fe^{3+} species (extra-framework) for the direct conversion of methane into methanol. Even a 5% increase in the proportion of this active species, especially when it exceeds 60%, can lead to a significant increase in activity. The chemical state and coordination environment of metal species in the catalysts were further investigated by X-ray fine structure analysis, XPS, and low-temperature Fourier transform infrared (LT-FTIR) spectroscopy with CO as a probe molecule. The Cu K-edge X-ray absorption near edge structure (XANES) spectrum of Cu-Fe(2/0.1)/ZSM-5 (Figure 2c) showed a pre-edge feature at 8977 eV, characteristic of Cu^{2+} species. The intensive white line feature centered at 8996 eV was attributed to the coordination of Cu^{2+} to H_2O or OH ligands.[5,31] The corresponding extended X-ray absorption fine structure (EXAFS, Figure S4 and Table S2) results indicated a Cu−O distance of 1.95 Å with a coordination number of 4 in the Cu-Fe(2/0.1)/ZSM-5 catalyst. The Fe K-edge XANES spectra of 0.1Fe/ZSM-5 and Cu-Fe(2/0.1)/ZSM-5 (Figure 2d) showed a pre-edge feature at ∼7115 eV, characteristic of Fe^{3+}.[25] The corresponding EXAFS data indicated two separate Fe−O shells, an Fe−O distance of 1.89 Å with a coordination number of 2 and an Fe−O distance of 2.05 Å with a coordination number of 4, corresponding to Fe−O−Al and Fe−OH/H_2O, respectively (Figure S4 and Table S3). Combined with our previous study,[22] the closest match between EXAFS data and theoretical modeling was obtained for the monomeric Fe complex $[(HO)_2 - Fe(III) - (H_2O)_2]^+$ containing two hydroxyl species as charge compensators and two coordinated Fe−O bonds with a zeolite framework, consistent with the lower R value of 1.89 Å in the Fe−O contribution. This structure thus is used to represent the resting state of the monomeric Fe species in ZSM-5 as shown in a later figure. The XPS analysis showed two peaks at 934.9 and 933.4 eV in the Cu $2p_{3/2}$ signal of Cu-Fe(2/0.1)/ZSM-5 (Figure 2e), indicative of the presence of isolated Cu hydroxyls located at the zeolite extra-framework and surface CuO nanoparticles, respectively.[32,33] An increase in the proportion of isolated Cu species was observed in Cu-Fe(2/0.1)/ZSM-5 compared to that in monometallic 2Cu/ZSM-5, indicating a larger amount of isolated Cu species inside the zeolite for the bimetallic catalyst. The coexistence of Cu^+ and Cu^{2+} species was further evidenced by the Cu LMM Auger spectra (Figure S5) with kinetic energies of 917.6 and 913.7 eV,[34,35] corroborated by LT-FTIR (Figure 2f), with the formation of Cu^+−CO species (2159 cm^{-1}) and $Cu^+-(CO)_2$ dicarbonyl species (2152 and 2180 cm^{-1}) at low CO pressures.[5,36] Therefore, the copresence of dominant isolated Fe and Cu species located at extra-framework of ZSM-5, and some CuO_x nanoparticles on the external surface of zeolite, was observed in the Cu-Fe(2/0.1)/ZSM-5 catalyst. The presence of Cu species slightly increases the proportion of monomeric Fe^{3+} species, facilitating methane activation. Simultaneously, the presence of Fe species promotes the dispersion of Cu species into the zeolite, in good accordance with the results of UV−vis DR (Figure 2a) and H_2 temperature-programmed reduction (H_2-TPR, Figure S6).

To account for the enhanced methanol selectivity observed for Cu-Fe(2/0.1)/ZSM-5, a time-on-line analysis was performed and compared with the two active Cu-Fe(2/0.1)/ZSM-5 and 0.1Fe/ZSM-5 catalysts, revealing different primary intermediates/products during methane oxidation (Figure 3a). For the 0.1Fe/ZSM-5 catalyst, CH_3OOH was the major intermediate and HCOOH was the main product. In contrast, CH_3OH was quickly produced and was stable as the main product for Cu-Fe(2/0.1)/ZSM-5, together with the suppression of the yield of CH_3OOH. The results clearly show that methane oxidation is affected by two different radical species, •OH and •OOH generated by the decomposition of H_2O_2 via two competitive pathways in parallel. To verify this, we prepared a solution with CH_3OOH as the primary component of C1 species by methane oxidation over 0.1Fe/ZSM-5 for 2 min, which was used as a substrate for CH_3OOH oxidation tests over the 0.1Fe/ZSM-5 and Cu-Fe(2/0.1)/ZSM-5 catalysts at a low temperature of 25 °C to slow down the reaction speed (Figure 3b,c). For 0.1Fe/ZSM-5, CH_3OOH decreased over time with a complete selectivity to HCOOH, indicating the preferential formation of HCOOH with 0.1Fe/ZSM-5 in CH_3OOH oxidation, consistent with the recent results that HCOOH is the main product for Fe-containing zeolite.[37] For the Cu-Fe(2/0.1)/ZSM-5 catalyst, the consumption of CH_3OOH and HCOOH was observed, owing to the quick overoxidation of HCOOH by •OH radicals. Notably, no CH_3OH increase was observed for both catalysts, suggesting that CH_3OH was not formed via CH_3OOH. Electron paramagnetic resonance (EPR) radical trapping studies (Figure 3d) showed that a limited amount of •OH radicals was detected over 0.1Fe/ZSM-5, indicating that Fe species exhibit limited contribution to the generation of •OH, while a significant amount of •OH radicals was formed over 2Cu/ZSM-5 and Cu-Fe(2/0.1)/ZSM-5, indicating that Cu species, instead of Fe species, facilitated the generation of •OH

https://doi.org/10.1021/acscatal.1c00905
ACS Catal. 2021, 11, 6684−6691

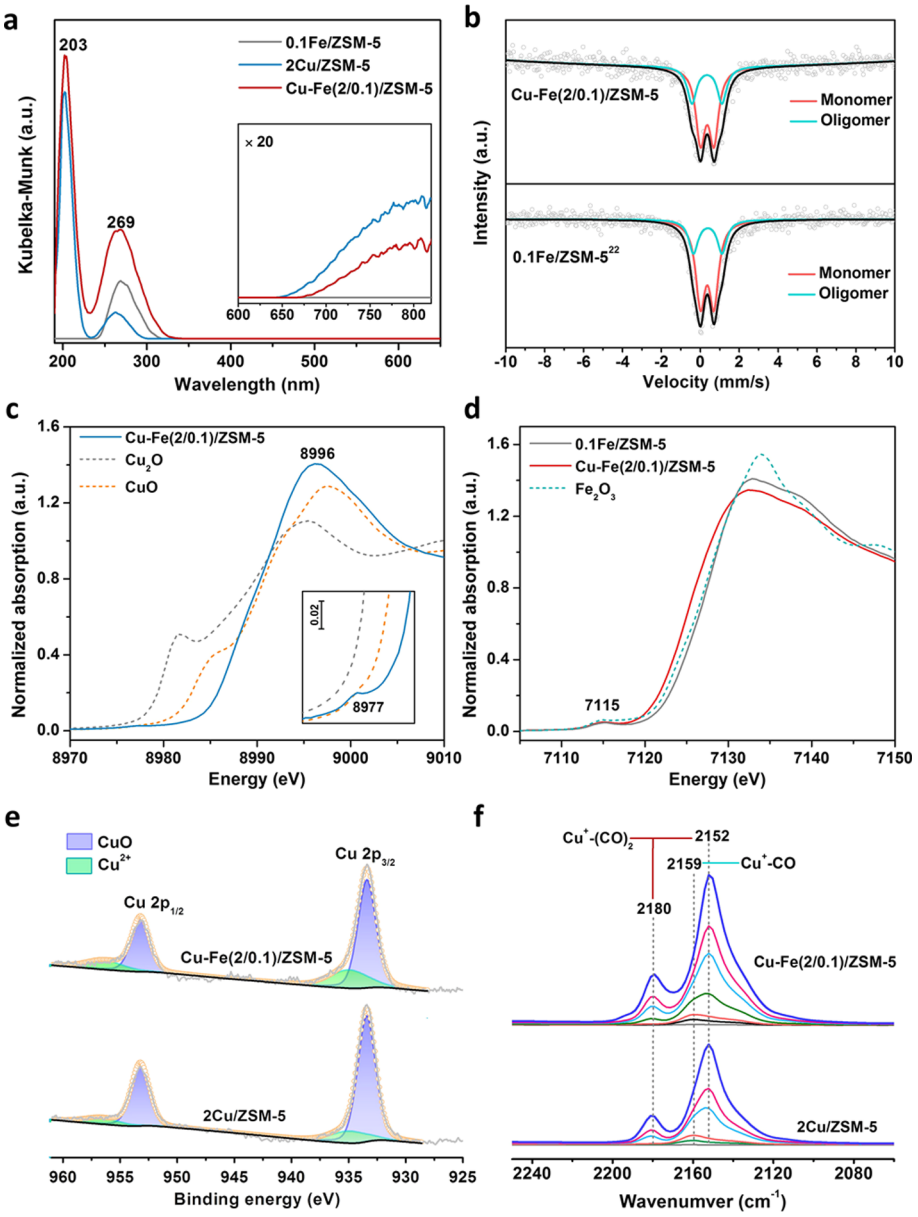

Figure 2. (a) UV−vis DR spectra of the different catalysts. (b) ^{57}Fe Mössbauer spectra at 298 K in air for 0.1Fe/ZSM-5[22] and Cu-Fe(2/0.1)/ZSM-5 samples. (c) Cu K-edge XANES spectrum of the Cu-Fe(2/0.1)/ZSM-5 catalyst. (d) Fe K-edge XANES spectra of 0.1Fe/ZSM-5 and Cu-Fe/ZSM-5 catalysts. (e) Cu 2p XPS spectra of 2Cu/ZSM-5 and Cu-Fe(2/0.1)/ZSM-5 catalysts. (f) Low-temperature FTIR spectra of CO absorbed over the 2Cu/ZSM-5 and Cu-Fe(2/0.1)/ZSM-5 catalysts at increasing equilibrium pressure from 1.4×10^{-4} to 8.6×10^{-2} mbar.

radicals from H_2O_2 decomposition. This is in excellent agreement with the results that Cu^{2+}/Cu^{+} species promote the selective decomposition of H_2O_2 into •OH radicals in the liquid phase.[19,20] Intriguingly, a quick consumption of •OH radicals was observed over Cu-Fe(2/0.1)/ZSM-5 after CH_4 addition into the reaction solution for 5 min (Figure 3e), accompanied by the production of a significant amount of CH_3OH (659 μmol, Figure 3a) yet no detection of $•CH_3$ radicals, suggesting that CH_3OH is primarily formed via immediate capture of as-generated $•CH_3$ species by significant quantities of •OH radicals.[23,26,38] As shown in Figure 3f, the pathway of methane oxidation by H_2O_2 proceeding with Cu-Fe(2/0.1)/ZSM-5 is predominantly via route 1 (colored in blue) in which methane is first activated on the isolated Fe sites to generate $•CH_3$ radicals, which subsequently react with the abundant •OH radicals facilitated by Cu species to form CH_3OH. Inevitably, partial oxidation of CH_3OH into $HOCH_2OOH$ or HCOOH and quickly to CO_2 was observed in the presence of oxidative •OH radicals (Figures S7,S8).[39] Contrastively, the pathway of methane oxidation over 0.1Fe/ZSM-5 is mainly via route 2 (colored in red in Figure 3f) in which methane is first activated on the isolated Fe sites to form $•CH_3$, which further reacts with •OOH to form CH_3OOH intermediate species and finally HCOOH as the major product over time, as the absence of Cu species mediates the shortage of •OH radicals in the solution during H_2O_2 decomposition.

DFT calculations were conducted to obtain detailed mechanistic insights into the selective oxidation of methane into CH_3OH over the Cu-Fe(2/0.1)/ZSM-5 catalyst in the aqueous solution of H_2O_2, as shown in Figure 4. Based on our experimental findings and previous study,[22] monomeric Fe^{3+} species predominantly in an octahedral coordination, hydrated

https://doi.org/10.1021/acscatal.1c00905
ACS Catal. 2021, 11, 6684−6691

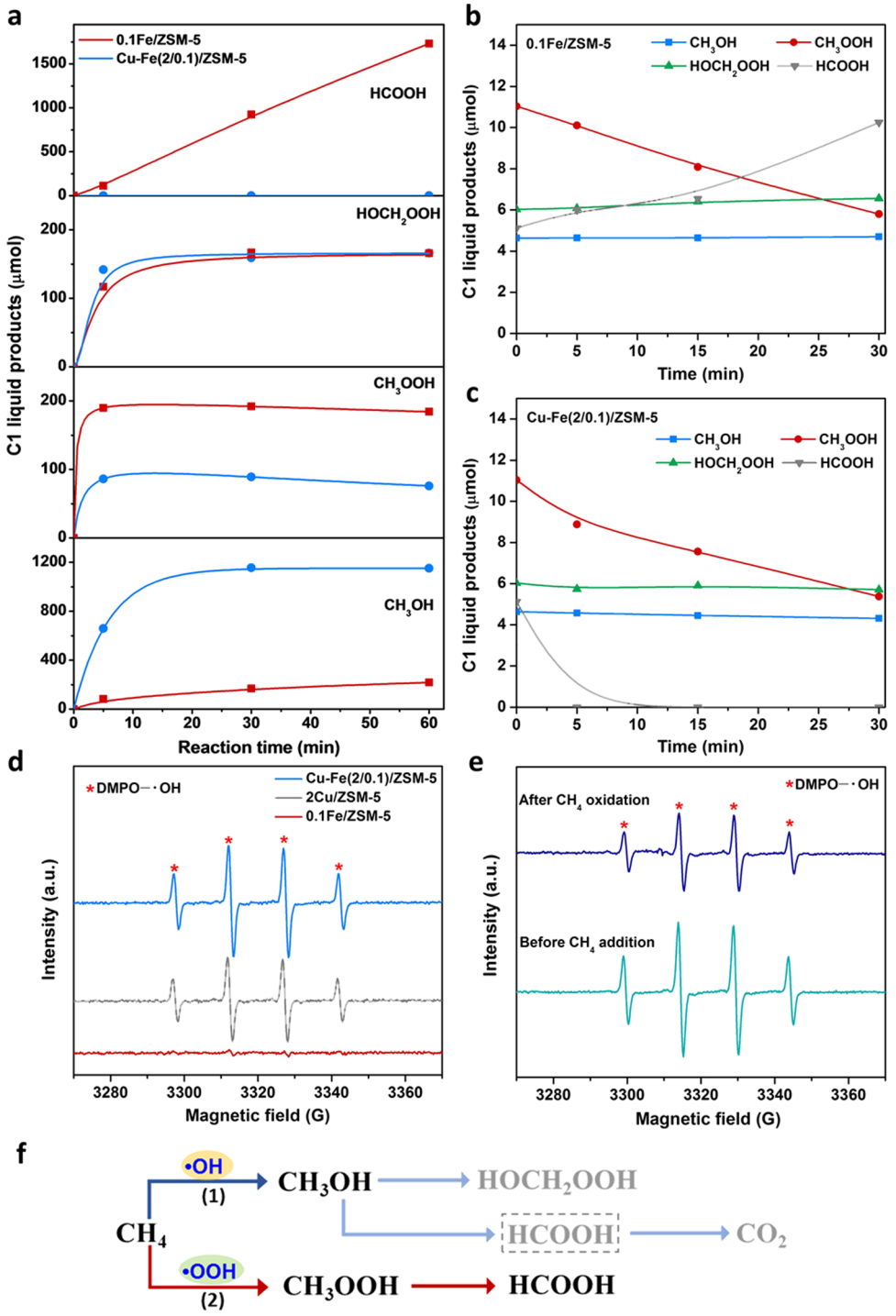

Figure 3. (a) Time-on-line profile for the reaction products of methane oxidation over the 0.1Fe/ZSM-5 and Cu-Fe(2/0.1)/ZSM-5 catalysts. (b,c) Time-on-line profile for C1 product oxidation over the 0.1Fe/ZSM-5 and Cu-Fe(2/0.1)/ZSM-5 catalysts. (d) EPR spectra obtained from a liquid sample after H_2O_2 decomposition over the 0.1Fe/ZSM-5, 2Cu/ZSM-5, and Cu-Fe(2/0.1)/ZSM-5 catalysts. (e) EPR trapping experiment with 5,5-dimethylpyrroline-*N*-oxide as the radical trapping agent over the Cu-Fe(2/0.1)/ZSM-5 catalyst with H_2O_2 as the oxidant. (f) Proposed reaction scheme for the oxidation of methane in a H_2O_2-based heterogeneous system.

$[(HO)_2{-}Fe(III){-}(H_2O)_2]^+$ complexes on the extra-framework of ZSM-5 as an initial active-site model (species **1**), and optimized structural models and intermediates are shown in Figures S9,S10. As shown in Figure 4, **1** first coordinates with H_2O_2 by substituting a water ligand, which weakly adsorbs on Fe^{3+}, to form species **2**. H^+ of adsorbed H_2O_2 transfers to the adjacent −OH ligand and then forms **3**. Noting that the Brønsted acid sites (BAS) can promote methane activation,[22] we delineate that the adjacent BAS indeed facilitates the cleavage of the peroxo (O−O) bond of Fe−OOH via dehydration of species **4** to form species **5** containing Fe(V)═O species. Methane is then adsorbed on **5** and forms species **6** followed by the homolytic dissociation of the C−H bond via a transient intermediate species (TS), which shows a reaction barrier of only 0.56 eV, exhibiting one of the lowest activation barriers for the Fe-containing zeolite catalysts

https://doi.org/10.1021/acscatal.1c00905
ACS Catal. 2021, 11, 6684−6691

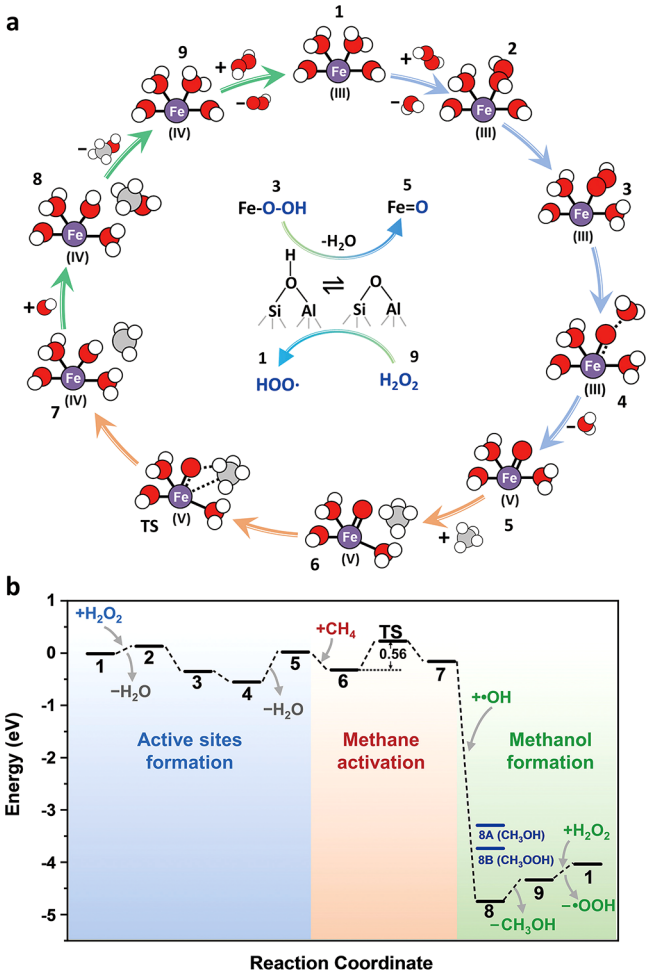

Figure 4. (a) Proposed reaction scheme of reaction pathway for direct methane oxidation to methanol over Cu-Fe(2/0.1)/ZSM-5 using H_2O_2 as the oxidant. Red, purple, gray, and white balls represent O, Fe, C, and H atoms, respectively. (b) DFT-simulated pathway on the mononuclear Fe^{3+} species in zeolite ZSM-5 for the oxidation of CH_4 to CH_3OH using H_2O_2, illustrating the thermodynamic feasibility of the proposed mechanism.

and indicating the preference and feasibility of the homolytic pathway for the intrinsic active species during methane activation.[18,23,40] After homolytic dissociation of the C−H bond, a $\bullet CH_3$ radical and a −OH ligand connected to the Fe site are formed. Upon CH_4 activation, one proton and one electron are transferred from methane to the active site, and the formal oxidation state of Fe(V) is reduced to Fe(IV) to form species **7**. Furthermore, we compared and studied the selectivity patterns with different catalysts after methane oxidation via possible routes. For the 0.1Fe/ZSM-5 catalyst, the $\bullet CH_3$ radicals are favorable to combine with •OOH radicals easily to form CH_3OOH (**8B**) thermodynamically, rather than combining with the −OH groups on the Fe center to generate CH_3OH (**8A**) through a rebound mechanism. This is in good agreement with the experimental results of CH_3OOH observed as the primary intermediate over 0.1Fe/ZSM-5, as shown in route 2 in Figure 3f. In contrast, the Cu species in Cu-Fe(2/0.1)/ZSM-5 promote H_2O_2 dissociation to generate a significant amount of •OH radicals with a barrier of only 0.08 eV, as shown in Figure S11. Subsequently, the abundant •OH radicals can readily combine with $\bullet CH_3$ radicals to form CH_3OH (**8**) directly, which is more exothermic than the generation of CH_3OOH, making methanol formation favorable in thermodynamics. Meanwhile, the *ab initio* molecular dynamics calculation results shown in Figure S12 show that the •OH radicals are beneficial to the decomposition of formic acid to CO_2. This result holds consistency with our experimental investigation that Cu species promote the generation of •OH radicals, which change the selectivity toward CH_3OH and simultaneously decompose formic acid, and the introduction of methane leads to obvious consumption of •OH radicals. After desorption of CH_3OH from species **8** to give species **9**, a second H_2O_2 molecule further adsorbs on the residual BAS, and BAS is regenerated via proton abstraction of the H_2O_2 molecule, where the initial active site **1** reforms and the catalytic cycle is closed. Our computational results confirm that mononuclear Fe species in the Cu-Fe(2/0.1)/ZSM-5 structure are mainly responsible for methane activation, and the Fe(V)═O active site can efficiently activate the C−H bond. Simultaneously, the well-dispersed Cu species promote the dissociation of H_2O_2 to generate abundant •OH radicals, which directly recombine with the as-generated $\bullet CH_3$ radicals to form methanol as the major product.

CONCLUSIONS

We have successfully prepared a highly efficient Cu-Fe(2/0.1)/ZSM-5 catalyst for the direct oxidation of methane into methanol, which shows a TOR of 431 $mol_{MeOH}{\cdot}mol^{-1}{}_{Fe}{\cdot}h^{-1}$ (with a methanol selectivity of 80%). Based on a combination of catalytic and spectroscopic measurements as well as theoretical calculations, we demonstrate that monomeric Fe species play a vital role in methane activation. The adjacent BAS facilitates the formation of an active Fe(V)═O intermediate via the dehydration of Fe−OOH in the aqueous H_2O_2 solution, enabling the homolytic cleavage of the primary C−H bond in a low-energy pathway to generate $\bullet CH_3$ radicals. Cu species in the Cu-Fe(2/0.1)/ZSM-5 catalyst play a key role in facilitating the formation of •OH radicals that quickly capture $\bullet CH_3$ radicals to form CH_3OH. The presence of •OH radicals makes methanol formation more favorable in thermodynamics, thus hindering the competitive route to form CH_3OOH and subsequently HCOOH. These findings provide valuable insights into the activation mechanism of methane oxidation under mild conditions and open up perspectives for designing highly efficient metal−zeolite heterogeneous catalysts for the selective activation of C−H bonds in light alkanes.

ASSOCIATED CONTENT

Supporting Information

The Supporting Information is available free of charge at https://pubs.acs.org/doi/10.1021/acscatal.1c00905.

Synthesis of Cu-Fe/ZSM-5 catalysts, catalyst testing procedure, and product quantification methods; elemental analysis and N_2 physisorption data; STEM, H_2-TPR, UV−vis, FTIR, XRD, XPS, EXAFS, ^{57}Fe Mössbauer, and EPR characterizations; and computational methods (PDF)

AUTHOR INFORMATION

Corresponding Authors

Weiyu Song − *State Key Laboratory of Heavy Oil Processing, China University of Petroleum, Beijing 102249, China;*

https://doi.org/10.1021/acscatal.1c00905
ACS Catal. 2021, 11, 6684−6691

orcid.org/0000-0001-5720-204X; Email: songwy@cup.edu.cn

Bert M. Weckhuysen − *Inorganic Chemistry and Catalysis group, Debye Institute for Nanomaterials Science, Utrecht University, Utrecht 3584 CG, The Netherlands;* orcid.org/0000-0001-5245-1426; Email: B.M.Weckhuysen@uu.nl

Wenhao Luo − *CAS Key Laboratory of Science and Technology on Applied Catalysis, Dalian Institute of Chemical Physics, Chinese Academy of Sciences, Dalian 116023, China;* orcid.org/0000-0003-1941-3799; Email: w.luo@dicp.ac.cn

Authors

Tao Yu − *CAS Key Laboratory of Science and Technology on Applied Catalysis, Dalian Institute of Chemical Physics, Chinese Academy of Sciences, Dalian 116023, China; University of Chinese Academy of Sciences, Beijing 100049, China;* orcid.org/0000-0001-9210-308X

Zhi Li − *State Key Laboratory of Heavy Oil Processing, China University of Petroleum, Beijing 102249, China*

Lu Lin − *CAS Key Laboratory of Science and Technology on Applied Catalysis, Dalian Institute of Chemical Physics, Chinese Academy of Sciences, Dalian 116023, China*

Shengqi Chu − *Institute of High Energy Physics, Chinese Academy of Sciences, Beijing 100049, China*

Yang Su − *CAS Key Laboratory of Science and Technology on Applied Catalysis, Dalian Institute of Chemical Physics, Chinese Academy of Sciences, Dalian 116023, China*

Aiqin Wang − *CAS Key Laboratory of Science and Technology on Applied Catalysis, Dalian Institute of Chemical Physics, Chinese Academy of Sciences, Dalian 116023, China; State Key Laboratory of Catalysis, Dalian Institute of Chemical Physics, Chinese Academy of Sciences, Dalian 116023, China;* orcid.org/0000-0003-4552-0360

Complete contact information is available at: https://pubs.acs.org/10.1021/acscatal.1c00905

Author Contributions

†T.L. and Z.L. contributed equally.

Notes

The authors declare no competing financial interest.

■ ACKNOWLEDGMENTS

Financial support for this work comes from the Strategic Priority Research Program of the Chinese Academy of Sciences (XDB17020100) and the Foundation of Dalian Institute of Chemical Physics (DICP I201915), which is gratefully acknowledged. We are also grateful for the support for X-ray absorption spectroscopy experiments from the Beijing Synchrotron Radiation Facility (BSRF).

■ REFERENCES

(1) Schwach, P.; Pan, X.; Bao, X. Direct Conversion of Methane to Value-Added Chemicals over Heterogeneous Catalysts: Challenges and Prospects. *Chem. Rev.* **2017**, *117*, 8497−8520.

(2) Ravi, M.; Ranocchiari, M.; van Bokhoven, J. A. The Direct Catalytic Oxidation of Methane to Methanol-A Critical Assessment. *Angew. Chem., Int. Ed.* **2017**, *56*, 16464−16483.

(3) Xie, S.; Lin, S.; Zhang, Q.; Tian, Z.; Wang, Y. Selective Electrocatalytic Conversion of Methane to Fuels and Chemicals. *J. Energy Chem.* **2018**, *27*, 1629−1636.

(4) Sun, L.; Wang, Y.; Guan, N.; Li, L. Methane Activation and Utilization: Current Status and Future Challenges. *Energy Technol.* **2020**, *8*, 1−13.

(5) Sushkevich, V. L.; Palagin, D.; Ranocchiari, M.; van Bokhoven, J. A. Selective Anaerobic Oxidation of Methane Enables Direct Synthesis of Methanol. *Science* **2017**, *356*, 523−527.

(6) Tang, P.; Zhu, Q.; Wu, Z.; Ma, D. Methane Activation: The Past and Future. *Energy Environ. Sci.* **2014**, *7*, 2580−2591.

(7) Meng, X.; Cui, X.; Rajan, N. P.; Yu, L.; Deng, D.; Bao, X. Direct Methane Conversion under Mild Condition by Thermo-, Electro-, or Photocatalysis. *Chem* **2019**, *5*, 2296−2325.

(8) Agarwal, N.; Freakley, S. J.; McVicker, R. U.; Althahban, S. M.; Dimitratos, N.; He, Q.; Morgan, D. J.; Jenkins, R. L.; Willock, D. J.; Taylor, S. H.; Kiely, C. J.; Hutchings, G. J. Aqueous Au-Pd Colloids Catalyze Selective CH_4 Oxidation to CH_3OH with O_2 under Mild Conditions. *Science* **2017**, *358*, 223−227.

(9) Liu, C. C.; Mou, C. Y.; Yu, S. S. F.; Chan, S. I. Heterogeneous Formulation of the Tricopper Complex for Efficient Catalytic Conversion of Methane into Methanol at Ambient Temperature and Pressure. *Energy Environ. Sci.* **2016**, *9*, 1361−1374.

(10) Banerjee, R.; Proshlyakov, Y.; Lipscomb, J. D.; Proshlyakov, D. A. Structure of the Key Species in the Enzymatic Oxidation of Methane to Methanol. *Nature* **2015**, *518*, 431−434.

(11) Ross, M. O.; MacMillan, F.; Wang, J.; Nisthal, A.; Lawton, T. J.; Olafson, B. D.; Mayo, S. L.; Rosenzweig, A. C.; Hoffman, B. M. Particulate Methane Monooxygenase Contains Only Mononuclear Copper Centers. *Science* **2019**, *364*, 566−570.

(12) Vanelderen, P.; Snyder, B. E. R.; Tsai, M.-L.; Hadt, R. G.; Vancauwenbergh, J.; Coussens, O.; Schoonheydt, R. A.; Sels, B. F.; Solomon, E. I. Spectroscopic Definition of the Copper Active Sites in Mordenite: Selective Methane Oxidation. *J. Am. Chem. Soc.* **2015**, *137*, 6383−6392.

(13) Kulkarni, A. R.; Zhao, Z.-J.; Siahrostami, S.; Nørskov, J. K.; Studt, F. Cation-Exchanged Zeolites for the Selective Oxidation of Methane to Methanol. *Catal. Sci. Technol.* **2018**, *8*, 114−123.

(14) Dinh, K. T.; Sullivan, M. M.; Serna, P.; Meyer, R. J.; Dincă, M.; Román-Leshkov, Y. Viewpoint on the Partial Oxidation of Methane to Methanol Using Cu- and Fe-Exchanged Zeolites. *ACS Catal.* **2018**, *8*, 8306−8313.

(15) Grundner, S.; Markovits, M. A. C.; Li, G.; Tromp, M.; Pidko, E. A.; Hensen, E. J. M.; Jentys, A.; Sanchez-Sanchez, M.; Lercher, J. A. Single-Site Trinuclear Copper Oxygen Clusters in Mordenite for Selective Conversion of Methane to Methanol. *Nat. Commun.* **2015**, *6*, 7546.

(16) Ravi, M.; Sushkevich, V. L.; Knorpp, A. J.; Newton, M. A.; Palagin, D.; Pinar, A. B.; Ranocchiari, M.; van Bokhoven, J. A. Misconceptions and Challenges in Methane-to-Methanol over Transition-Metal-Exchanged Zeolites. *Nat. Catal.* **2019**, *2*, 485−494.

(17) Raynes, S.; Shah, M. A.; Taylor, R. A. Direct Conversion of Methane to Methanol with Zeolites: Towards Understanding the Role of Extra-Framework d-Block Metal and Zeolite Framework Type. *Dalton Trans.* **2019**, *48*, 10364−10384.

(18) Hammond, C.; Forde, M. M.; Ab Rahim, M. H.; Thetford, A.; He, Q.; Jenkins, R. L.; Dimitratos, N.; Lopez-Sanchez, J. A.; Dummer, N. F.; Murphy, D. M.; Carley, A. F.; Taylor, S. H.; Willock, D. J.; Stangland, E. E.; Kang, J.; Hagen, H.; Kiely, C. J.; Hutchings, G. J. Direct Catalytic Conversion of Methane to Methanol in an Aqueous Medium by Using Copper-Promoted Fe-ZSM-5. *Angew. Chem., Int. Ed.* **2012**, *51*, 5129−5133.

(19) Lyu, L.; Zhang, L.; Wang, Q.; Nie, Y.; Hu, C. Enhanced Fenton Catalytic Efficiency of γ-Cu-Al_2O_3 by σ-Cu^{2+}-Ligand Complexes from Aromatic Pollutant Degradation. *Environ. Sci. Technol.* **2015**, *49*, 8639−8647.

(20) Li, H.; Cheng, R.; Liu, Z.; Du, C. Waste Control by Waste: Fenton−like Oxidation of Phenol over Cu Modified ZSM−5 from Coal Gangue. *Sci. Total Environ.* **2019**, *683*, 638−647.

(21) Sun, Y.; Tian, P.; Ding, D.; Yang, Z.; Wang, W.; Xin, H.; Xu, J.; Han, Y. F. Revealing the Active Species of Cu-Based Catalysts for

Heterogeneous Fenton Reaction. *Appl. Catal. B* **2019**, *258*, No. 117985.
(22) Yu, T.; Li, Z.; Jones, W.; Liu, Y.; He, Q.; Song, W.; Du, P.; Yang, B.; An, H.; Farmer, D. M.; Qiu, C.; Wang, A.; Weckhuysen, B. M.; Beale, A. M.; Luo, W. Identifying Key Mononuclear Fe Species for Low-Temperature Methane Oxidation. *Chem. Sci.* **2021**, *12*, 3152−3160.
(23) Cui, X.; Li, H.; Wang, Y.; Hu, Y.; Hua, L.; Li, H.; Han, X.; Liu, Q.; Yang, F.; He, L.; Chen, X.; Li, Q.; Xiao, J.; Deng, D.; Bao, X. Room-Temperature Methane Conversion by Graphene-Confined Single Iron Atoms. *Chem* **2018**, *4*, 1902−1910.
(24) Kalamaras, C.; Palomas, D.; Bos, R.; Horton, A.; Crimmin, M.; Hellgardt, K. Selective Oxidation of Methane to Methanol over Cu- and Fe-Exchanged Zeolites: The Effect of Si/Al Molar Ratio. *Catal. Lett.* **2016**, *146*, 483−492.
(25) Hammond, C.; Dimitratos, N.; Jenkins, R. L.; Lopez-Sanchez, J. A.; Kondrat, S. A.; Hasbi ab Rahim, M.; Forde, M. M.; Thetford, A.; Taylor, S. H.; Hagen, H.; Stangland, E. E.; Kang, J. H.; Moulijn, J. M.; Willock, D. J.; Hutchings, G. J. Elucidation and Evolution of the Active Component within Cu/Fe/ZSM-5 for Catalytic Methane Oxidation: From Synthesis to Catalysis. *ACS Catal.* **2013**, *3*, 689−699.
(26) Zhao, W.; Shi, Y.; Jiang, Y.; Zhang, X.; Long, C.; An, P.; Zhu, Y.; Shao, S.; Yan, Z.; Li, G.; Tang, Z. Fe-O Clusters Anchored on Nodes of Metal-Organic Frameworks for Direct Methane Oxidation. *Angew. Chem., Int. Ed.* **2021**, *60*, 5811−5815.
(27) Li, Y.; Deng, J.; Song, W.; Liu, J.; Zhao, Z.; Gao, M.; Wei, Y.; Zhao, L. Nature of Cu Species in Cu-SAPO-18 Catalyst for NH_3-SCR: Combination of Experiments and DFT Calculations. *J. Phys. Chem. C* **2016**, *120*, 14669−14680.
(28) Sultana, A.; Nanba, T.; Haneda, M.; Sasaki, M.; Hamada, H. Influence of Co-Cations on the Formation of Cu^+ Species in Cu/ZSM-5 and Its Effect on Selective Catalytic Reduction of NO_x with NH_3. *Appl. Catal. B* **2010**, *101*, 61−67.
(29) Schwidder, M.; Kumar, M. S.; Klementiev, K.; Pohl, M. M.; Brückner, A.; Grünert, W. Selective Reduction of NO with Fe-ZSM-5 Catalysts of Low Fe Content: I. Relations between Active Site Structure and Catalytic Performance. *J. Catal.* **2005**, *231*, 314−330.
(30) Pérez-Ramírez, J.; Groen, J. C.; Brückner, A.; Kumar, M. S.; Bentrup, U.; Debbagh, M. N.; Villaescusa, L. A. Evolution of Isomorphously Substituted Iron Zeolites during Activation: Comparison of Fe-Beta and Fe-ZSM-5. *J. Catal.* **2005**, *232*, 318−334.
(31) Brezicki, G.; Kammert, J. D.; Gunnoe, T. B.; Paolucci, C.; Davis, R. J. Insights into the Speciation of Cu in the Cu-H-Mordenite Catalyst for the Oxidation of Methane to Methanol. *ACS Catal.* **2019**, *9*, 5308−5319.
(32) Platzman, I.; Brener, R.; Haick, H.; Tannenbaum, R. Oxidation of Polycrystalline Copper Thin Films at Ambient Conditions. *J. Phys. Chem. C* **2008**, *112*, 1101−1108.
(33) Feng, X.; Cao, Y.; Lan, L.; Lin, C.; Li, Y.; Xu, H.; Gong, M.; Chen, Y. The Promotional Effect of Ce on CuFe/Beta Monolith Catalyst for Selective Catalytic Reduction of NO_x by Ammonia. *Chem. Eng. J.* **2016**, *302*, 697−706.
(34) Kong, J.; Rui, Z.; Liu, S.; Liu, H.; Ji, H. Homeostasis in Cu_xO/$SrTiO_3$ Hybrid Allows Highly Active and Stable Visible Light Photocatalytic Performance. *Chem. Commun.* **2017**, *53*, 12329−12332.
(35) Zhen, W.; Jiao, W.; Wu, Y.; Jing, H.; Lu, G. The Role of a Metallic Copper Interlayer during Visible Photocatalytic Hydrogen Generation over a $Cu/Cu_2O/Cu/TiO_2$ Catalyst. *Catal. Sci. Technol.* **2017**, *7*, 5028−5037.
(36) Giordanino, F.; Vennestrøm, P. N. R.; Lundegaard, L. F.; Stappen, F. N.; Mossin, S.; Beato, P.; Bordiga, S.; Lamberti, C. Characterization of Cu-Exchanged SSZ-13: A Comparative FTIR, UV-Vis, and EPR Study with Cu-ZSM-5 and Cu-β with Similar Si/Al and Cu/Al Ratios. *Dalton Trans.* **2013**, *42*, 12741−12761.
(37) Zhu, K.; Liang, S.; Cui, X.; Huang, R.; Wan, N.; Hua, L.; Li, H.; Chen, H.; Zhao, Z.; Hou, G.; Li, M.; Jiang, Q.; Yu, L.; Deng, D. Highly Efficient Conversion of Methane to Formic Acid under Mild Conditions at ZSM-5-Confined Fe-Sites. *Nano Energy* **2021**, *82*, No. 105718.
(38) Shen, Q.; Cao, C.; Huang, R.; Zhu, L.; Zhou, X.; Zhang, Q.; Gu, L.; Song, W. Single Chromium Atoms Supported on Titanium Dioxide Nanoparticles for Synergic Catalytic Methane Conversion under Mild Conditions. *Angew. Chem., Int. Ed.* **2020**, *59*, 1216−1219.
(39) Taran, O. P.; Yashnik, S. A.; Ayusheev, A. B.; Piskun, A. S.; Prihod'ko, R. V.; Ismagilov, Z. R.; Goncharuk, V. V.; Parmon, V. N. Cu-Containing MFI Zeolites as Catalysts for Wet Peroxide Oxidation of Formic Acid as Model Organic Contaminant. *Appl. Catal. B* **2013**, *140-141*, 506−515.
(40) Szécsényi, Á.; Li, G.; Gascon, J.; Pidko, E. A. Mechanistic Complexity of Methane Oxidation with H_2O_2 by Single-Site Fe/ZSM-5 Catalyst. *ACS Catal.* **2018**, *8*, 7961−7972.

https://doi.org/10.1021/acscatal.1c00905
ACS Catal. 2021, 11, 6684−6691